Electronic and magnetic properties of 3*d* transition-metal atom adsorbed graphene and graphene nanoribbons

H. Sevinçli,[1] M. Topsakal,[2] E. Durgun,[1] and S. Ciraci[1,2,*]
[1]*Department of Physics, Bilkent University, 06800 Ankara, Turkey*
[2]*UNAM, Institute of Materials Science and Nanotechnology, Bilkent University, 06800 Ankara, Turkey*
(Received 27 March 2008; revised manuscript received 23 April 2008; published 22 May 2008)

In this paper, we theoretically studied the electronic and magnetic properties of graphene and graphene nanoribbons functionalized by 3*d* transition-metal (TM) atoms. The binding energies and electronic and magnetic properties were investigated for the cases where TM atoms adsorbed to a single side and double sides of graphene. We found that 3*d* TM atoms can be adsorbed on graphene with binding energies ranging between 0.10 and 1.95 eV depending on their species and coverage density. Upon TM atom adsorption, graphene becomes a magnetic metal. TM atoms can also be adsorbed on graphene nanoribbons with armchair edge shapes (AGNR's). Binding of TM atoms to the edge hexagons of AGNR yields the minimum energy state for all TM atom species examined in this work and in all ribbon widths under consideration. Depending on the ribbon width and adsorbed TM atom species, AGNR, which is a nonmagnetic semiconductor, can either be a metal or a semiconductor with ferromagnetic or antiferromagnetic spin alignment. Interestingly, Fe or Ti adsorption makes certain AGNR's half-metallic with a 100% spin polarization at the Fermi level. Present results indicate that the properties of graphene and graphene nanoribbons can be strongly modified through the adsorption of 3*d* TM atoms.

DOI: 10.1103/PhysRevB.77.195434 PACS number(s): 72.80.Rj, 72.25.−b, 73.61.Wp, 75.75.+a

I. INTRODUCTION

After the synthesis of isolated single graphene,[1] research interest has shifted to its unique properties and potential applications (see Ref. 2, and references therein). Among those properties are the anomalous quantized Hall effect,[3] "massless" Dirac electrons near the *K* point,[3] and the high mobility of carriers, which allows ballistic transport properties at submicron scale, at room temperature.[1] Graphene nanoribbons (GNR's) are of special interest due to their potential electronic and spintronic applications. A variety of methods were proposed or demonstrated in order to functionalize GNR's for new device applications[4–10] such as gas sensors,[4] spin-valve devices,[5,6] and resonant tunneling devices.[7] Experimental realization of GNR's near atomic precision was achieved[11] and their width and geometry dependent electronic properties were extensively studied.[5,12–17] Following the literature, we call GNR's that have an armchair edge shape with N_a dimer lines as N_a-AGNR's.

Earlier works using tight binding method[12] showed that electronic properties of GNR's are strongly dependent on their edge shapes as well as on their widths. Density functional theory[18] (DFT) calculations showed that[10] hydrogen passivated AGNR's are direct band gap semiconductors and that their band gaps follow three different curves depending on the value of N_a. For a given integer n, $N_a=3n+1$ has the highest band gap, whereas $N_a=3n-1$ has the lowest. As n increases, all these curves approach zero without crossing each other. The width dependent band gaps make AGNR's interesting candidates as building blocks of future electronic devices. Throughout this paper we refer to the hydrogen terminated AGNR's unless stated otherwise.

This work presents a detailed study of the magnetic and electronic properties of 3*d* transition-metal (TM) adsorbed graphene and AGNR's using density functional theory. The equilibrium geometries and electronic and magnetic properties are obtained using state-of-the-art *ab initio* total energy DFT calculations.[19] We found that TM atom decorated graphene shows different magnetic properties depending on the concentration and the species of TM atoms. For single TM atom adsorption to a unit cell of AGNR, the strongest binding occurs when the TM atom is adsorbed above the center of the edge hexagon. In the case of two TM atoms per unit cell, the second TM atom prefers the hollow site of the neighboring hexagon so as to form a zigzag chain of TM atoms at the edge of the AGNR. The magnetic properties of those species having strong binding are loosely affected by the ribbon width. Also, the adsorption of Fe and Ti to AGNR gives rise to half-metallic band structures.

II. ADSORPTION OF TRANSITION-METAL ATOMS ON GRAPHENE

Here, we investigate the electronic and magnetic properties of graphene when Co, Cr, Fe, Mn, or Ti atoms are adsorbed. We consider different coverages of TM atoms, such as one TM atom adsorbed on either (2×2) or (4×4) unit cells on only one side as well as on both sides, namely, above and below the graphene. The geometrical configurations of the structures under consideration are represented in Figs. 1(a) and 1(b). Three different adsorption sites in the single-sided adsorption to (2×2) cell are considered. These consist of the hollow site (H1) being above the center of the hexagon, the bridge site (B1) over a C-C bond, and the top site (T1) directly above a C atom [see Fig. 1(a)]. For double-sided adsorption, wherein a TM atom is adsorbed on a H1 site from above, there are three more inequivalent possible sites B2, H2, and T2, as illustrated in Fig. 1(a).

First, we discuss our results for the single-sided adsorption on the (2×2) cell. For all TM atoms under consider-

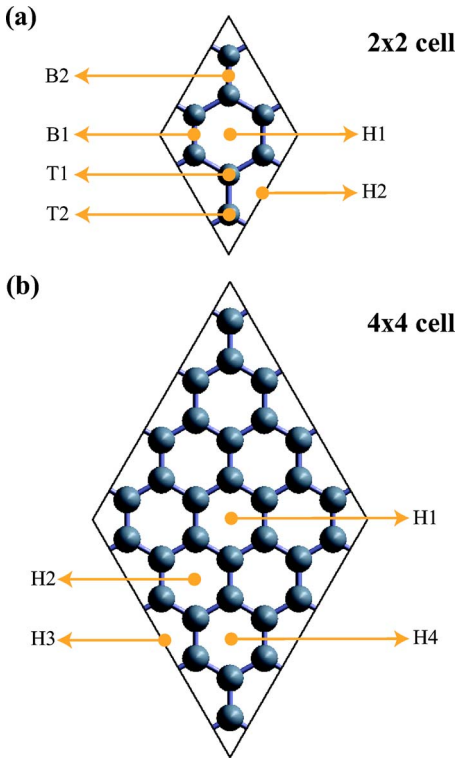

FIG. 1. (Color online) (a) A (2×2) cell of graphene and the six possible adsorption sites for the TM atoms. B1, H1, and T1 are the single-sided adsorption sites, whereas B2, H2, and T2 are the possible additional sites for the double-sided adsorption. (b) A (4×4) cell of graphene and the four sites we consider for the adsorption of the second TM atom from below when the first TM atom is adsorbed on H1 from above. Calculations have been performed by using supercell geometry and hence the above adsorption geometries have been periodically repeated in two dimensions.

ation, binding to the H1 site is energetically more favorable except for Cr, which prefers the B1 site. In order to check the magnetic state of the structure, we double the previous geometry in both directions and set the initial magnetic moments of TM atoms to be antiferromagnetic (AFM).

In Table I, we summarize the minimum energy geometries and the magnetic states of the single-sided adsorption on the (2×2) graphene cell, the corresponding binding energies, and total magnetic moments of the systems. The total magnetic moments of the minimum energy states and the distance of the TM atom to the nearest carbon atom are also included in Table I. The binding energies are calculated as $E_b=E[\text{graphene}]+E[\text{TM}]-E[(\text{graphene}+\text{TM})]$ in terms of the total energies of the bare graphene per (2×2) cell ($E[\text{graphene}]$), the free TM atom in its ground state ($E[\text{TM}]$), and one TM atom adsorbed on a (2×2) cell of graphene ($E[\text{graphene}]+E[\text{TM}]$). All total energies are calculated in the same supercell, keeping all the other parameters of the calculation fixed. The coupling between the TM atoms, which is significant for the (2×2) cell calculations and hence weakens the TM-graphene binding, is subtracted from E_b. On the other hand, the TM-TM coupling is weaker in the case of a single atom adsorbed on the (4×4) cell; however, the TM-graphene binding becomes stronger. Note that the decoration by TM atoms, where one TM atom is adsorbed on each periodically repeating (4×4) cell of graphene, can represent an isolated TM atom adsorbed on graphene. We see that Cr and Mn do not have a considerable binding for any of the configurations. Their binding energies are 0.18 and 0.10 eV, respectively. Both Cr and Mn prefer AFM ground states. Binding energies of Ti, Co, and Fe are relatively stronger and all prefer the H1 site. For Ti, the minimum energy magnetic state is AFM, whereas for Co or Fe adsorbed graphene, it is ferromagnetic (FM) with magnetic moments $1.31\mu_B$ (Bohr magneton) and $3.02\mu_B$, respectively.

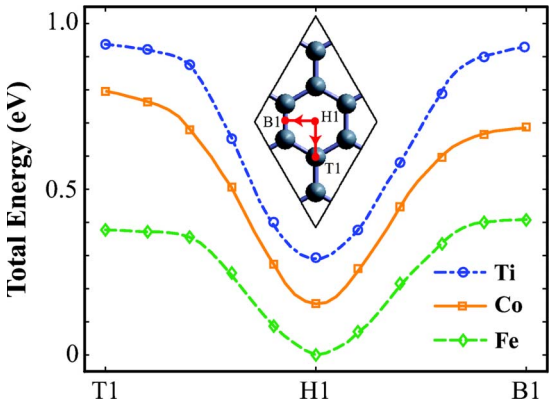

FIG. 2. (Color online) Analysis of the energetics of Ti, Co, and Fe moving from H1 to T1 and from H1 to B1. The transient paths are given in the inset. Total energy of the unit cell is plotted for each path ($H1\rightarrow T1, H1\rightarrow B1$), which is divided into sections with equal lengths.

A few words about the states other than the minimum energy state are necessary to complete the discussion. First,

TABLE I. Minimum energy adsorption sites and magnetic states (either FM or AFM) for single-sided adsorption of one TM atom adsorbed per (2×2) cell. The binding energies (E_b), the total magnetic moments μ_{tot}, and the distances to the nearest C atom (d) are also listed. The binding energy of a single TM atom adsorbed on a (4×4) cell is given in parentheses for the sake of comparison.

	Ti H1 AFM	Co H1 FM	Fe H1 FM	Cr B1 AFM	Mn H1 AFM
E_b (eV)	1.58 (1.95)	1.20 (1.27)	0.66 (1.02)	0.18 (0.20)	0.10 (0.17)
μ_{tot} (μ_B)	0.0	1.31	3.02	0.0	0.00
d (Å)	2.32	2.12	2.21	2.39	2.47

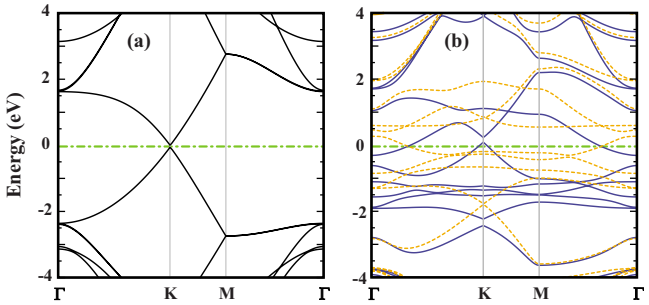

FIG. 3. (Color online) (a) Band structure of the bare graphene calculated for the (2×2) cell. (b) Band structure for one Co adsorbed on each (2×2) cell of graphene. Blue (dark) and orange (light) curves indicate the majority and minority spin bands, respectively. The zero of the energy is set to the Fermi energy.

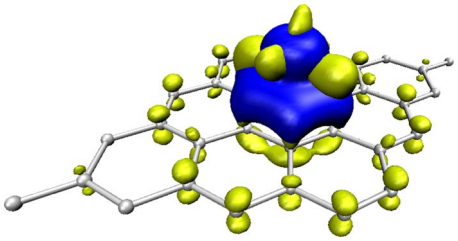

FIG. 4. (Color online) Spin resolved charge accumulation (i.e., $\Delta\rho_{\uparrow(\downarrow)}>0$) obtained from the charge density difference calculation for one Ti atom adsorbed on each (4×4) cell of graphene (see the text). Blue (dark) and yellow (light) regions indicate the isosurfaces of majority and minority spin states, respectively.

the top site never yields a ground state for any of the TM atoms. No matter where the Co atom is initially placed (bridge, hollow, or top site), it always finds its minimum energy state at the hollow H1 site after relaxation for both FM and AFM cases. On the other hand, Cr, Fe, Mn, and Ti, which are initially placed at the T1 site within the FM state, remain at the T1 site upon the relaxation of the structure. Fe and Ti atoms, when they are placed at the T1 site in the AFM state, drift to the H1 site and subsequently dimerize to occupy neighboring hexagons.

We further examined the energy of the system when the TM atom is restricted to be adsorbed to sites on the lines from H1 to T1, and from B1 to H1 for Co, Fe, and Ti.[24] In Fig. 2, the total energies of adsorption to the sites on the lines T1-H1 and H1-B1 are given. The energy minimum occurs at H1, whereas the energy barriers ΔQ for adsorption to T1 are 0.38, 0.64, and 0.74 eV for Fe, Co, and Ti, respectively, and those for adsorption to B1 are ΔQ=0.41, 0.53, and 0.74 eV, respectively. Accordingly, the diffusion of adsorbed Ti to form a cluster is prevented by a significant potential barrier of 0.74 eV. However, the diffusion of Fe is relatively easy.

The band structures of the TM atom adsorbed on the (2×2) graphene cell indicate that the systems are FM metallic for Co and Fe, while AFM metallic for Ti, Cr, and Mn. We compare the band structures of the bare graphene folded according to the Brillouin zone of a (2×2) cell with that of one Co atom adsorbed on each (2×2) graphene cell (Fig. 3). As a result of Co adsorption, new bands originating from Co cross the Fermi energy and the bands of underlying graphene are modified. Consequently, the density of states at E_F increases and the metallicity of graphene is enhanced.

In the double-sided adsorption, we tested six different sites for the second TM atom, keeping the first one at the H1 site. By considering FM and AFM configurations for the above and below TM atoms, we employed ionic relaxation. In Table II, the minimum energy configurations and the binding energies for the adsorption of the second TM atom, total magnetic moments of the structures, and the distances of the TM atoms to the nearest carbon atoms are listed. For Ti, Co, Fe, and Mn, the energetically favorable adsorption site for the second TM atom is the H2 site. The binding energies for the below Ti and Mn atoms are larger than that of the single-sided adsorption, and their equilibrium positions are closer. On the contrary, for Co and Fe, the binding energies decrease and their distances to the C atoms increase. The analysis of the total magnetic moments indicates that for Co and Fe, the above and below TM atoms have opposite magnetic moments; however, for Ti, the net magnetic moment is finite but small. Mn atoms have parallel magnetic moments. Since not only the TM-graphene interaction but also the TM-TM interaction is effective in lowering the total energy of the system, one may expect the TM atoms to prefer the adsorption site which enables the closest TM-TM distance possible. In double-sided adsorption, the smallest TM-TM distance is achieved by adsorption of both TM atoms on the same hollow site from above and below. Our calculations show that such a configuration is not favorable energetically. Even though the TM-TM interaction lowers the total energy, the

TABLE II. Minimum energy geometries and magnetic states for double-sided adsorption of two TM atoms adsorbed per (2×2) cell. The binding energies (E_b), the total magnetic moments (μ_{tot}), and the distances of above (d) and below (d') TM atoms to the nearest C atom are listed. The binding energies in parentheses correspond to the single-sided adsorption of one TM atom on each (4×4) cell.

	Ti H2 FM	Co H2 AFM	Fe H2 AFM	Cr B2 FM	Mn H2 FM
E_b (eV)	1.79	1.11	0.60	0.33	0.26
	(1.95)	(1.27)	(1.02)	(0.20)	(0.17)
μ_{tot} (μ_B)	0.14	0.0	0.0	0.16	9.77
d (Å)	2.28	2.18	2.24	2.41	2.46
d' (Å)	2.28	2.18	2.24	2.32	2.47

TABLE III. Adsorption sites and corresponding magnetic states (FM or AFM), binding energies (E_b), total magnetic moments (μ_{tot}), and nearest carbon distances (d and d') for double-sided adsorption of one TM atom adsorbed on each (4×4) cell from above and below. The first TM atom is adsorbed on the H1 site from above.

	Ti H2 AFM	Co H3 FM	Fe H4 FM	Cr H2 AFM	Mn H3 FM
$E_{b,\text{above}}$ (eV)	1.95	1.27	1.02	0.18	0.17
$E_{b,\text{below}}$ (eV)	2.27	1.27	1.08	0.19	0.25
μ_{tot} (μ_B)	0.0	2.0	4.0	0.02	10.49
d (Å)	2.26	2.10	2.09	2.53	2.50
d' (Å)	2.26	2.10	2.08	2.55	2.53

TM-graphene interaction is also affected by the adsorption of both TM atoms by the same carbon atoms. Consequently, the minimum energy states are those with TM atoms adsorbed on H2 for Ti, Co, Fe, and Mn, and on B2 for Cr.

We also investigate the double-sided adsorption of two TM atoms on the (4×4) cell. We examined the adsorption of the second TM atom on H2, H3, and H4 sites from below when the first TM atom is sitting above the H1 site [see Fig. 1(b)]. The minimum energy configurations with binding energies and the total magnetic moments are given in Table III. We note that the tradeoff between the TM-TM interaction and the TM-graphene interaction in double-sided adsorption on a (2×2) cell also holds for the double-sided adsorption on a (4×4) cell.

The binding properties of TM atoms on graphene are further analyzed by calculating the charge density difference of majority ($\uparrow$) and minority ($\downarrow$) spin states, i.e., $\Delta\rho_{\uparrow(\downarrow)}=\rho_{\uparrow(\downarrow)}[\text{graphene+Ti}]-\rho_{\uparrow(\downarrow)}[\text{graphene}]-\rho_{\uparrow(\downarrow)}[\text{Ti}]$ in the (4×4) unit cell. Here, $\rho_{\uparrow(\downarrow)}[\text{graphene+Ti}]$ is the total charge of the majority and minority spin states of one Ti atom adsorbed on each (4×4) cell of graphene. $\rho_{\uparrow(\downarrow)}[\text{graphene}]$ and $\rho_{\uparrow\downarrow}[\text{Ti}]$ are the charge densities of noninteracting bare graphene and Ti atom that have the same positions as in the case of graphene and adsorbed Ti. All charge densities have been calculated in the same supercell. The plotted isosurfaces in Fig. 4 show the accumulation of majority and minority spin charge densities as a result of the adsorption of Ti in comparison to noninteracting constituents. The isosurface plot shows an increase in majority spin density between graphene and Ti and a net increase in minority spin electrons on Ti. The difference in majority and minority spin densities demonstrates the induced magnetization on $2p_z$ orbitals of hexagon atoms.

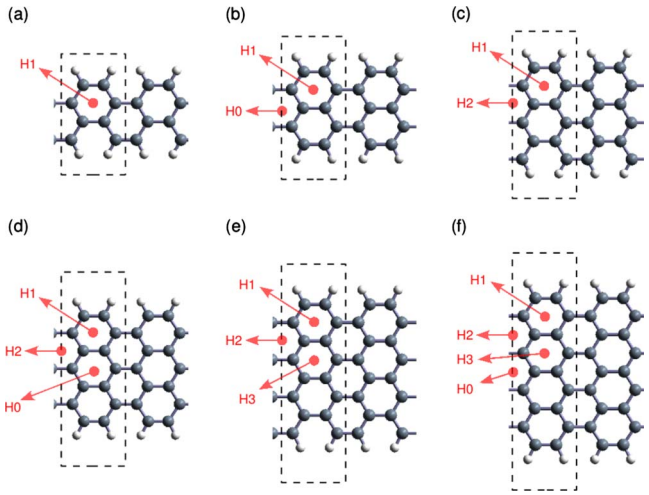

FIG. 5. (Color online) (a)–(f) possible hollow sites for adsorption on AGNR's with N_a=4, 5, 6, 7, 8, and 9. For all N_a, H1 is the edge hollow site. H0 appears for N_a=5, 7, and 9, which indicates that the middle hollow site fulfills the reflection symmetry. H2 and H3 are the remaining sites if they are different from the previous ones, with H2 being closer to H1. The unit cells are indicated by dashed lines.

III. ADSORPTION OF TRANSITION-METAL ATOMS ON GRAPHENE NANORIBBONS

In this section, we present the spin dependent properties of TM atom (Co, Cr, Fe, Mn, and Ti) adsorbed on AGNR's.

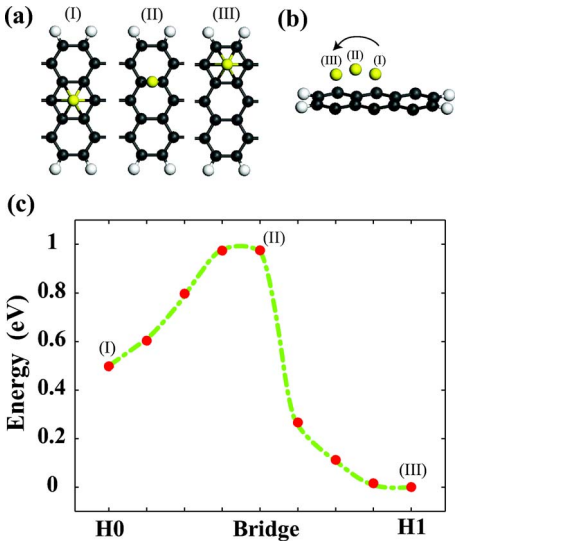

FIG. 6. (Color online) Transition state analysis of Ti adsorbed on 7-AGNR between H0 and H1 sites above the bridge site. (a) Top view of three adsorption sites of Ti on 7-AGNR from H0 to H1, i.e., H0, bridge, and H1 sites are shown. (b) Side view for these three adsorption sites. Adsorption to the C-C bridge gives the farthest position to the AGNR plane. (c) Total energy per unit cell for Ti adsorption on the path from H0 to H1 (see the text).

TABLE IV. Binding energies to possible sites of N_a-AGNR shown in Fig. 5 (in units of eV).

		Ti	Co	Fe	Cr	Mn
4-AGNR	H1	2.22	1.29	1.15	0.32	0.36
5-AGNR	H0	2.16	1.12	0.97	0.38	0.25
	H1	2.29	1.37	1.14	0.52	0.43
6-AGNR	H1	2.22	1.31	1.19	0.36	0.35
	H2	1.90	1.02	0.79	0.24	0.24
7-AGNR	H0	1.84	0.90	0.72	0.23	0.03
	H1	2.24	1.29	1.17	0.38	0.35
	H2	2.02	1.06	0.91	0.24	0.08
8-AGNR	H1	2.27	1.36	1.17	0.45	0.37
	H2	2.07	1.07	0.92	0.32	0.16
	H3	1.97	1.10	0.87	0.33	0.15
9-AGNR	H0	1.99	1.08	0.94	0.25	0.07
	H1	2.24	1.32	1.18	0.38	0.35
	H2	1.95	1.05	0.84	0.26	0.06
	H3	1.90	1.02	0.79	0.25	0.01

We examine the variation of electronic and magnetic properties of AGNR's with different widths. The dependence on the concentration of TM atoms and the effect of adsorption on different sites are examined in order to understand the variations and the origins of the magnetic properties. We define the TM atom coverage θ as the number of TM atoms per cell, and we study the cases with $\theta=1$ and 2.

We first calculated the electronic structure of AGNR's with different widths and obtained consistent results with the earlier first-principles calculations.[10] Now we consider the $\theta=1$ coverage, where a single TM atom is adsorbed per unit cell of AGNR. Due to the broken symmetry along the transverse direction, the number of possible adsorption sites increases with the width of the ribbon. We examined the hollow sites for the adsorption of all five species for AGNR's with $N_a=4$, 5, 6, 7, 8, and 9. The adsorption sites under consideration are shown in Fig. 5. For all AGNR's considered, H1 is the hollow site at the very edge of the AGNR. H0 is the hollow site with equal distances to both edges and exists for $N_a=2n+1$ only ($n\geq 2$). H2 and H3 are the remaining hollow sites, which are not equivalent to H0 or H1, with H2 being closer to H1. The binding energies to these sites are given in Table IV.

For all TM species and for all AGNR's of different widths under consideration, H1 is the energetically most favorable site for adsorption at $\theta=1$. For $N_a=7$, the second preferable site is H2 for all species. In $N_a=9$ case, H0 becomes the second minimum energy adsorption site except for Cr, which prefers H2. When $N_a=8$, H3 has less energy than H2 for Co and Cr, whereas Mn and Ti have H2 as the second preferable

TABLE V. The magnetic ground states of TM atom adsorbed N_a-AGNR depending on TM coverage (θ), the width (N_a), and the adsorption site as described in Fig. 5. (AFM)FM-M(S), (antiferromagnetic) ferromagnetic metal (semiconductor); HM, half-metal. Zigzag coverage for $\theta=2$ refers to the zigzag chain of TM atoms at the edge of the ribbon as explained in the text.

N_a	θ	site	Ti	Co	Fe	Cr	Mn
4	1	H1	FM-M	FM-M	FM-M	AFM-S	AFM-S
	2	Zigzag	FM-HM	FM-M	FM-S	AFM-M	AFM-M
5	1	H1	FM-M	FM-S	AFM-S	AFM-M	AFM-M
	1	H0	FM-M	FM-M	FM-S	FM-M	AFM-M
	2	Zigzag	FM-HM	FM-M	FM-HM	FM-M	FM-M
6	1	H1	FM-M	FM-M	AFM-S	AFM-S	FM-M
	2	Zigzag	FM-M	FM-M	FM-M	FM-M	FM-M
7	1	H1	FM-M	FM-M	FM-M	AFM-S	AFM-S
	1	H0	FM-M	FM-M	FM-M	FM-M	AFM-M
8	1	H1	FM-M	FM-M	FM-HM	AFM-S	AFM-S
9	1	H1	FM-M	FM-M	AFM-S	AFM-M	FM-M
	1	H0	FM-M	FM-HM	FM-S	FM-M	AFM-M

adsorption site. Another difference between adsorption on AGNR and adsorption on graphene is that the TM atoms stabilize their binding by gaining some displacement out of the center of the edge hexagon. This displacement has different values for different species, but, as a rule of thumb, the stronger the binding, the smaller the displacement.

Next, we analyze the transition state energies for 7-AGNR on the path from H0 to H1 over a bridge site as seen in Figs. 6(a) and 6(b).[25,26] The total energies of these configurations are plotted in Fig. 6(c). The energy barrier from H0 to H1 is $\Delta Q_{H0\rightarrow H1}=0.48$ eV, while it is $\Delta Q_{H1\rightarrow H0}=0.97$ eV in the reverse direction. These results suggest that the diffusion of adsorbed Ti atoms to form a cluster is hindered by a significant energy barrier ΔQ.

The magnetic states of H1-adsorbed AGNR's fall into two categories. Co and Ti adsorption produces FM metals for all widths of AGNR's, and Cr adsorption produces AFM semiconductors with band gaps ranging between 0.07 and 0.56 eV depending on the ribbon width.[27] On the other hand, Mn and Fe adsorptions do not exhibit that robust character. Fe adsorbed AGNR's are FM metals for $N_a=4$ and $N_a=7$, half-metallic with an energy gap of 0.12 eV for minority spin for $N_a=8$, and AFM semiconductor for $N_a=5$, $N_a=6$, and $N_a=9$. Mn adsorbed 6-AGNR is a FM metal, while for other N_a, Mn adsorbed AGNR's are AFM semiconductors with energy band gaps ranging between 0.40 and 0.69 eV. We observe that the species with strongest binding, i.e., Ti and Co, alter the semiconducting character of AGNR's to FM metals, while those with weakest binding (Cr and Mn) cannot metallize the ribbons and they generally prefer AFM alignment.

We also check the magnetic ground states of adsorption to H0 site of $\theta=1$. H0 site is of special importance because of its mirror symmetry in the transverse direction, and it exists only for $N_a=2n+1$ with $n\geq 2$. The TM atom adsorbed on H0 site is at equal distance to the edges. Therefore, one may expect the quantum interferences in this special geometry to have effects on the adsorption properties. Interestingly, for Ti, Co, Fe, and Cr, the minimum energy states are always FM, and for Mn, it is AFM.

For $\theta=2$ adsorption, we consider one TM atom to be adsorbed on the H1 site and the other on the H2 site, which lowers the energy by TM-TM dimerization. We calculate three cases $N_a=4$, 5, and 6 in order to sample the three families of AGNR's. For all cases, the zigzag chains of TM atoms at the edges either metallize the AGNR's or give rise to half-metallicity. We find that the zigzag chain of Fe on 5-AGNR is half-metallic, with an energy gap of 0.10 eV for minority spin [Fig. 7(b)]. Similarly, Ti zigzag chains on 4- and 5-AGNR are half-metallic with energy gaps of 0.05 and 0.16 eV, respectively, for majority spin [Fig. 7(c)]. Accordingly, TM-adsorbed AGNR is metallic for one spin direction, but it is semiconductor for the opposite spin direction. Net spin in the unit cell is an integer and the spin polarization at the Fermi level (i.e., $P=|D_{\uparrow}(E_F)-D_{\downarrow}(E_F)|/[D_{\uparrow}(E_F)+D_{\downarrow}(E_F)]$ in terms of the density of states at E_F for each spin state, namely, $D_{\uparrow(\downarrow)}(E_F)$) is 100%. The calculated magnetic and electronic states of TM-adsorbed AGNR's of $\theta=1$ and 2 are summarized in Table V. As seen, the electronic structures and magnetic states show dramatic variations depending on the adsorbate, the adsorption site, the adsorbate coverage (θ), and the width of the AGNR (N_a).

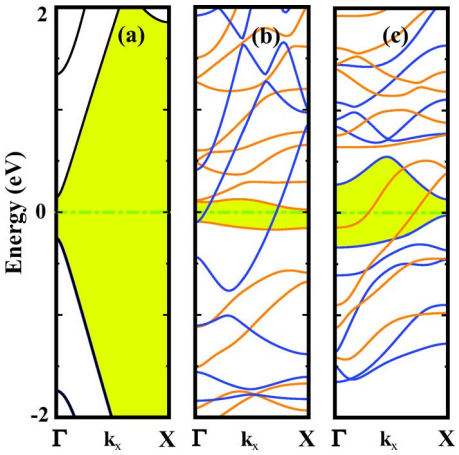

FIG. 7. (Color online) (a) Band structures of 5-AGNR and $\theta=2$ coverages of 5-AGNR (b) with Fe and (c) with Ti. Fermi energy is set to zero. In (b) and (c), blue (dark) curves are the bands with majority spin, and orange (light) curves are the bands with minority spin. Fe adsorption opens a gap of 0.10 eV for the minority spin, while the majority spin is metallic. Adsorption of Ti makes the minority spin metallic, while the majority spin has an energy gap of 0.16 eV at the Fermi energy.

IV. CONCLUSION

In summary, we study the electronic and magnetic properties and binding characters of TM atom adsorbed on graphene and armchair graphene nanoribbons. For graphene, it is found that adsorption on the hollow site gives the minimum energy for all TM atoms we examined except for Cr. The possibility of dimerization of two TM atoms adsorbed on adjacent unit cells for AFM states is also investigated. For Ti, Co, and Fe, dimerization is weaker, whereas for Mn and Cr, it is more pronounced. The same applies to AGNR's, where the edge hollow site yields the minimum energy. Upon TM atom adsorption, semimetallic bare graphene can change to a ferromagnetic or antiferromagnetic metal. The electronic and magnetic properties of TM atom adsorbed armchair graphene nanoribbons show variations depending on the adsorbate concentration, adsorption site, and the species of TM elements. In general, their magnetic states are more robust for strongly binding species in the sense that their magnetic properties are less altered by the ribbon width. This makes them candidates for future applications, especially for wider ribbons. Also, zigzag chain formation of adsorbed TM atoms at the ribbon edge makes AGNR's an interesting system for studying magnetism in one dimension.

ACKNOWLEDGMENTS

This research was supported in part by TÜBİTAK through TR-Grid e-Infrastructure Project and by the National Center for High Performance Computing of Turkey, Istanbul Technical University through Grant No. 2-024-2007.

*ciraci@fen.bilkent.edu.tr

[1] K. S. Novoselov, A. K. Geim, S. V. Morozov, D. Yiang, Y. Zhang, S. V. Dubonos, I. V. Grigorieva, and A. A. Firsov, Science **306**, 666 (2004).
[2] A. K. Geim and K. S. Novoselov, Nat. Mater. **6**, 183 (2007).
[3] K. S. Novoselov, A. K. Geim, S. V. Morozov, D. Jiang, M. I. Katsnelson, I. V. Grigorieva, S. V. Dubonos, and A. A. Firsov, Nature (London) **438**, 197 (2005); Y. Zhang, Y.-W. Tan, H. L. Stormer, and P. Kim, *ibid.* **438**, 201 (2005).
[4] F. Schedin, A. K. Geim, S. V. Morozov, E. W. Hill, P. Blake, M. I. Katsnelson, and K. S. Novoselov, Nat. Mater. **6**, 652 (2007).
[5] T. B. Martins, R. H. Miwa, A. J. R. da Silva, and A. Fazzio, Phys. Rev. Lett. **98**, 196803 (2007).
[6] M. Topsakal, H. Sevinçli, and S. Ciraci, Appl. Phys. Lett. **92**, 173118 (2008).
[7] H. Sevinçli, M. Topsakal, and S. Ciraci, arXiv:0711.2414 (unpublished).
[8] E. Rudberg, P. Salek, and Y. Luo, Nano Lett. **7**, 2211 (2007).
[9] Y.-W. Son, M. L. Cohen, and S. G. Louie, Nature (London) **444**, 347 (2006); see also **446**, 342 (2007).
[10] Y.-W. Son, M. L. Cohen, and S. G. Louie, Phys. Rev. Lett. **97**, 216803 (2006); see also **98**, 089901(E) (2007).
[11] X. Li, X. Wang, L. Zhang, S. Lee, and H. Dai, Science **319**, 1229 (2008).
[12] M. Fujita, K. Wakabayashi, K. Nakada, and K. Kusakabe, J. Phys. Soc. Jpn. **65**, 1920 (1996).
[13] L. Pisani, J. A. Chan, B. Montanari, and N. M. Harrison, Phys. Rev. B **75**, 064418 (2007).
[14] K. Nakada, M. Fujita, G. Dresselhaus, and M. S. Dresselhaus, Phys. Rev. B **54**, 17954 (1996).
[15] Y. Miyamoto, K. Nakada, and M. Fujita, Phys. Rev. B **59**, 9858 (1999).
[16] M. Ezawa, Phys. Rev. B **73**, 045432 (2006).
[17] E. H. Lieb, Phys. Rev. Lett. **62**, 1201 (1989).
[18] W. Kohn and L. J. Sham, Phys. Rev. **140**, A1133 (1965); P. Hohenberg and W. Kohn, Phys. Rev. **136**, B864 (1964).
[19] We use a projected augmented wave (Ref. 20) approach within a PW91 (Ref. 21) -GGA (Ref. 22) approximation for the exchange and correlation functionals as currently implemented in the VASP (Ref. 23) software. Geometry optimizations for bulk structures are performed by allowing all atomic positions and all cell parameters to vary. All atomic positions are optimized by the conjugate gradient method and the system is considered to be at equilibrium when Hellman–Feynman forces are below 10 meV/Å. We use a Monkhorst–Pack mesh with a sufficient number of k points to converge the energies. For one-dimensional and two-dimensional structures, (21, 1, 1) and (11, 11, 1) k-point meshes, respectively, are implemented. Periodic boundary conditions are implemented in all directions, where a sufficiently large vacuum (minimum of 10 Å) is inserted in directions without crystal symmetry in order to prevent artificial interactions. The kinetic energy cutoff for the plane wave basis set is chosen as $\hbar^2|\mathbf{k}+\mathbf{G}|^2/2m=500$ eV and the convergence criterion for electronic relaxations has been set to 10^{-5} eV.
[20] P. E. Blöchl, Phys. Rev. B **50**, 17953 (1994).
[21] J. P. Perdew, J. A. Chevary, S. H. Vosko, K. A. Jackson, M. R. Pederson, D. J. Singh, and C. Fiolhais, Phys. Rev. B **46**, 6671 (1992).
[22] J. P. Perdew, K. Burke, and M. Ernzerhof, Phys. Rev. Lett. **77**, 3865 (1996).
[23] G. Kresse and J. Hafner, Phys. Rev. B **47**, 558 (1993); G. Kresse and J. Furthmuller, *ibid.* **54**, 11169 (1996).
[24] During the relaxation of ionic positions, the x and y coordinates of the TM atom are fixed and the z coordinate is left free. Also, the farthest C atom is fixed in the cell in order to ensure the relative position of the TM atom with respect to the underlying graphene.
[25] We choose nine equidistant points along the path. During relaxation, we fix the y and z coordinates of the closest carbon atoms forming the C-C bridge and x and y coordinates of the Ti atom for each configuration, leaving the rest of the coordinates free.
[26] E.-J. Kan, H. J. Xiang, J. Yang, and J. G. Hou, J. Chem. Phys. **127**, 164706 (2007).
[27] We note that the DFT method underestimates the band gaps found in this work (Ref. 28). However, this situation does not affect our conclusions in any essential manner.
[28] L. Yang, C.-H. Park, Y.-W. Son, M. L. Cohen, and S. G. Louie, Phys. Rev. Lett. **99**, 186801 (2007).